Synthesis, solubility and thermodynamic properties of N-A-S-H gels with various target Si/Al ratios

Chen, Yun; de Lima, Luiz Miranda; Li, Zhenming; Ma, Bin; Lothenbach, Barbara; Yin, Suhong; Yu, Qijun; Ye, Guang

DOI
10.1016/j.cemconres.2024.107484

Publication date
2024

Document Version
Final published version

Published in
Cement and Concrete Research

Citation (APA)
Chen, Y., de Lima, L. M., Li, Z., Ma, B., Lothenbach, B., Yin, S., Yu, Q., & Ye, G. (2024). Synthesis, solubility and thermodynamic properties of N-A-S-H gels with various target Si/Al ratios. *Cement and Concrete Research*, *180*, Article 107484. https://doi.org/10.1016/j.cemconres.2024.107484

Cement and Concrete Research 180 (2024) 107484

Contents lists available at ScienceDirect

Cement and Concrete Research

journal homepage: www.elsevier.com/locate/cemconres

Synthesis, solubility and thermodynamic properties of N-A-S-H gels with various target Si/Al ratios

Yun Chen [a,b], Luiz Miranda de Lima [b], Zhenming Li [c,f], Bin Ma [d], Barbara Lothenbach [e], Suhong Yin [a], Qijun Yu [a], Guang Ye [b,*]

[a] School of Materials Science and Engineering, South China University of Technology, Guangzhou 510640, Guangdong, China
[b] Section of Materials and Environment, Faculty of Civil Engineering and Geosciences, Delft University of Technology, Delft 2628CN, the Netherlands
[c] School of Civil and Environmental Engineering, Harbin Institute of Technology, 518055 Shenzhen, China
[d] Laboratory for Waste Management, Paul Scherrer Institut (PSI), Forschungsstrasse 111, 5232 Villigen, Switzerland
[e] Concrete & Asphalt Laboratory, Swiss Federal Laboratories for Materials Science and Technology (Empa), Dübendorf 8600, Switzerland
[f] Guangdong Provincial Key Laboratory of Intelligent and Resilient Structures for Civil Engineering, Harbin Institute of Technology, 518055 Shenzhen, China

ARTICLE INFO

Keywords:
N-A-S-H gel
Solubility product
Thermodynamic properties
Si/Al ratio
Sol-gel method

ABSTRACT

The synthesis of N-A-S-H gel with high Si/Al ratios (>2) has been rarely reported in the literature, leaving the establishment of a reliable synthesis route as an open challenge. This paper aims to synthesize N-A-S-H gels with Si/Al ratios ranging from 1 to 3 and establish their thermodynamic database. The effects of reaction temperature, reaction time, initial Si/Al, concentration of reactants and pH of the matrix on the Si/Al ratios of the synthesized N-A-S-H gel were investigated. Results showed that N-A-S-H gels with target Si/Al ratios can be synthesized by controlling the concentration of reactants, pH and initial Si/Al ratios. The solubility products of the obtained N-A-S-H gels were determined via dissolution tests at different temperatures, to determine thermodynamic data. The development of this experimentally derived thermodynamic database of N-A-S-H gels constitutes a crucial step in the advancement of thermodynamic modeling of geopolymer, providing valuable insight into geopolymer reactions and phase assemblages.

1. Introduction

Geopolymer stands out as an eco-friendly cementitious binder due to its lower carbon emissions and comparable engineering properties compared with ordinary Portland cement. The main reaction product in geopolymer is generally sodium aluminosilicate hydrate (N-A-S-H) gel [1–3]. N-A-S-H gels can be described as a 3D network of tetrahedral Si and Al linked by bridging oxygens, with Na^+ chemically bonded to compensate for the negative charge of tetrahedral Al [4–6]. The chemical composition of N-A-S-H gel can be written as $Na^+[AlO_2{\cdot}nSiO_2]^-{\cdot}mH_2O$, where the most important variable Si/Al ratio, n, can range from 1 to 3 [7], depending on the raw materials [8] and the curing regime [9]. As the principal phase, N-A-S-H gel dictates the microstructure and thus the engineering properties of geopolymers. A thermodynamic database of N-A-S-H gels, including the solubility products and other thermodynamic properties, are indispensable for studying the chemical reactions involved in geopolymerization. However, the available thermodynamic database for N-A-S-H gels is scarce and incomplete. So far, the thermodynamic properties of N-A-S-H gels, i.e. the Gibbs free energy, heat capacity, entropy, enthalpy, and molar volume, have been rarely reported, which hinders the investigation of reactions and phase assemblages of geopolymers through thermodynamic modeling.

The solubility products of N-A-S-H gels are the key parameters that determine their thermodynamic properties. Generally, there are two approaches to experimentally derive the solubility of a solid in aqueous phase, i.e., from oversaturation state and from undersaturation state. The former refers to determining the ion concentrations in equilibrium from an oversaturation state [10,11], while the latter is through the dissolution of a pre-synthesized pure phase [12–14]. Only few studies employed the first approach to measure the solubility products of N-A-S-H gels. Williamson et al. [10,11] conducted a study on the solubility products of N-A-S-H gels under an oversaturation state at 50 °C till 56 days. However, the solid residue obtained from the samples was found to be amorphous only for the initial 3 days. After that, it was converted into faujasite, which could affect the solubility results of N-A-S-H gels. Using

* Corresponding author.
E-mail address: G.Ye@tudelft.nl (G. Ye).

https://doi.org/10.1016/j.cemconres.2024.107484
Received 31 May 2023; Received in revised form 8 February 2024; Accepted 20 March 2024
Available online 28 March 2024

pre-synthesis of N-A-S-H gels is more common to determine their solubility. Walkley et al. [13] synthesized N-A-S-H gels with Si/Al ratios ranging from 1 to 2 through the alkali-activation of synthetic aluminosilicate precursor. However, several crystalline phases like α-$Al(OH)_3$ and faujasite-Na were detected in the products. As a result, the dissolution test was conducted on impure N-A-S-H gels, which could also interfere with the result. Pure N-A-S-H gels with Si/Al ratios ranging from 1 to 2 were obtained using sol-gel method [12], which is the most commonly used method to synthesize a single phase of N-A-S-H gel. After that, the N-A-S-H gels were equilibrated with water at 25 °C and 50 °C. The solubility products of N-A-S-H gels reported in the literature [11–13] are summarised in Table A1. However, it is not possible to directly compare these data due to differences either in the chemical formula of N-A-S-H gel or the dissolution reaction. Overall, the reliability of these results remains uncertain, particularly considering the potential effect of impurities.

The experimentally derived solubility product of N-A-S-H gel with a Si/Al ratio higher than 2 has not been reported, although the Si/Al ratio of N-A-S-H gel in geopolymer pastes most likely falls in the range of 2–3 [9,15,16]. In order to complete the solubility data of N-A-S-H gels with various Si/Al ratios in the geopolymer system, synthesis of pure N-A-S-H gel with a Si/Al ratio up to 3 is needed to further determine its solubility product. However, few studies managed a Si/Al ratio up to 3. Even worse, the reported Si/Al ratio of synthesized N-A-S-H gels [11,12,17] are partially contradictory. While N-A-S-H gel with a Si/Al ratio of around 2 was successfully synthesized using an initial Si/Al ratio of 2 in [12,17], Williamson et al. [11] reported a Si/Al ratio in N-A-S-H gel around 1 with the same initial ratio. Furthermore, they managed to obtain high Si/Al N-A-S-H gel by using an initial Si/Al ratio up to 9.6, but only achieved a Si/Al ratio of 2.4 [11]. These results indicate that synthesizing high Si/Al N-A-S-H gel could be a challenging task.

There is no standard procedure for synthesis of N-A-S-H gels, as demonstrated by varying conditions used in [11,12,17,18], while the effects of these reaction conditions on the resulting N-A-S-H gels are still unknown. For instance, the synthesis of N-A-S-H gel has been conducted at different temperature, ranging from 2 to 5 °C [12,17], room temperature [18], to as high as 50 °C [11], and lasted for different reaction time, varying from 1 day [17] to 7 days [12]. Additionally, largely different concentrations of reactants have been used to synthesize N-A-S-H gel, with 0.1 M sodium silicate and aluminum nitrate solutions used in [17] and much higher solutions (1 M) used in [18]. Besides, it has been suggested to synthesize N-A-S-H gel at high pH (> 12.5) to avoid the formation of silica gel at low pH [18]. However, Williamson et al. [11] found that using a higher Si/Na ratio within the reactants, corresponding to lower pH values, was helpful to form N-A-S-H gel with a higher Si/Al ratio. In order to synthesize N-A-S-H gels with various Si/Al ratios, the effects of these synthesis conditions on the resulting N-A-S-H gels, especially their chemical compositions, need to be clarified.

The main purpose of this study is to establish a procedure to synthesize N-A-S-H gels covering a range of Si/Al ratio from 1 to 3, and to investigate their solubility and thermodynamic properties. Firstly, the synthesis mixtures and conditions reported in the literature were employed to investigate their effect on the synthetic N-A-S-H gels, whose chemical compositions were determined by X-ray fluorescence analysis (XRF) and mass balance calculations, while the structural information was gained from X-ray diffraction (XRD) and Fourier transform infrared spectroscopy (FTIR). Next, modified recipes were developed, with the underlying mechanisms analyzed. The optimal route to synthesize N-A-S-H gels was proposed. The target N-A-S-H gels were characterized using XRF, scanning electron microscopy with energy dispersive X-ray spectroscopy (SEM-EDX), thermogravimetric analysis (TGA), XRD and FTIR. Dissolution experiment of N-A-S-H gels was conducted at different temperatures to determine their solubility products. The obtained results were compared with the solubility products of zeolites and N-A-S-H gels from literature. The effect of Si/Al ratio in N-A-S-H gel on its solubility was discussed. Finally, thermodynamic properties of N-A-S-H gels were derived from the experimentally determined solubility product at 25 °C, and validated by the solubility products measured at high temperatures. This comprehensive study is expected to provide valuable insights into the synthesis, solubility, and thermodynamic properties of N-A-S-H gels with various Si/Al ratios.

2. Experimental method

2.1. Synthesis of N-A-S-H gel

Different concentrations of sodium silicate solutions (0.1 M, 0.2 M, 0.3 M and 1 M) and aluminum nitrate solutions (0.1 M and 1 M) were prepared using deionized water with $Na_2SiO_3{\cdot}5H_2O$ (AR-grade) and $Al(NO_3)_3{\cdot}9H_2O$ (AR-grade), respectively. A 10 M NaOH solution and a HNO_3 solution (>65 %, Honeywell) were used as pH regulators if necessary. The sodium silicate solution was first mixed with the pH regulator and stirred for 30 mins. Aluminum nitrate solution was then added dropwise to the stirring solution. A total of 15 synthesis systems were studied in this work, covering five influencing factors, i.e. reaction time, reaction temperature, initial Si/Al ratio, concentration of reactants and pH of the matrix. Detailed synthesis conditions for all samples are given in Table 1. In order to examine the synthesis mixtures and conditions in literature [11,12,17], samples G1, G2, G3, G3_7days, G3_ice and G10 were prepared with 0.1 M aluminum nitrate solution and different concentrations of sodium silicate solutions. Among them, G1, G2, G3 and G10 were designed to study the effect of initial Si/Al, G3_7days was reacted for 7 days at 20 °C to study the effect of reaction time, and G3_ice was placed in an ice-bath (2–5 °C) for 1 day to study the effect of reaction temperature. Samples G3_lc, G3_mc and G3_hc were prepared by using different concentrations of reactants to study the effect of concentration, while G3_hc_mpH and G3_hc_lpH were synthesized by adding different amounts of HNO_3 solution to investigate the effect of pH. Note that the above procedure took place in a N_2-filled glove box to avoid carbonation.

After stirring for 1 day (or 7 days), the suspension was centrifuged at 5000 rpm for 5 min to separate the solid reaction product, i.e. gel, and liquid. The liquid was filtered using a 0.45 μm syringe filter to be further analyzed. The gel was triple-washed by fully dispersing in deionized water to remove nitrates and unbound sodium, followed by 100 ml of >96 vol% ethanol solution for the last wash. The amount of washing water was found to affect the measured Na/Al of the gels significantly. Na/Al ratio in the N-A-S-H gel is supposed to be 1 in theory. In this work, at least 1500 ml of washing water was used to obtain a reasonable Na/Al ratio. Note that the amount of washing water should be adjusted according to the amount of synthesized solid gels. In the end, the gel was dried in a vacuum desiccator using saturated $CaCl_2$ solution as a desiccant for 14 days. When relative humidity reaches equilibrium, i.e. ~33 %, the gels were removed for further characterization. Note that at least two duplicate samples were made for each mixture and the average results were presented.

2.2. Characterization

After synthesis, two parts were obtained: gel and filtrate. Characterization of gel was performed by XRF, XRD, FTIR, EDX and TGA [18,19]. XRF measurement was performed with a Panalytical Axios Max WD-XRF spectrometer on loose powder. XRD analysis was carried out on a Bruker D8 Advance diffractometer at 45 KV and 40 mA using CuKα radiation. The powder samples were scanned from 8° to 60° 2θ at a rate of 2 s per step and a step size of 0.02° 2θ. FTIR characterization was conducted using Nicolet™ iS50 FTIR Spectrometer over the wavelength range of 600 to 4000 cm^{-1} with a resolution of 4 cm^{-1}. The samples were examined for the elemental compositions by EDX measurements using a Philips XL30 SEM equipped with NSS3.3. The EDX measurements were carried out at an accelerating voltage of 10 kV in the high vacuum mode. Approximately 10 mg of N-A-S-H gel powder was

Table 1
Synthesis mixtures and conditions.

Samples[a]	Na_2SiO_3	$Al(NO_3)_3$	Concentration of Si	Concentration of Al	pH regulator	Reaction time	Reaction temperature	Target Si/Al	pH[b]
G1	200 ml 0.1 M	200 ml 0.1 M	0.048 M	0.048 M	20 ml 10 M NaOH	1 day	20 °C	1	13.53
G2	200 ml 0.2 M	200 ml 0.1 M	0.095 M	0.048 M	20 ml 10 M NaOH	1 day	20 °C	2	13.60
G3	200 ml 0.3 M	200 ml 0.1 M	0.143 M	0.048 M	20 ml 10 M NaOH	1 day	20 °C	3	13.68
G3_7days	200 ml 0.3 M	200 ml 0.1 M	0.143 M	0.048 M	20 ml 10 M NaOH	7 days	20 °C	3	13.72
G3_ice	200 ml 0.3 M	200 ml 0.1 M	0.143 M	0.048 M	20 ml 10 M NaOH	1 day	2–5 °C	3	13.70
G10	100 ml 1 M	100 ml 0.1 M	0.45 M	0.045 M	10 ml 10 M NaOH	1 day	20 °C	3	13.87
G3_lc_n	200 ml 0.3 M	200 ml 0.1 M	0.15 M	0.05 M	–	1 day	20 °C	3	12.93
G3_mc_n	200 ml 0.3 M	20 ml 1 M	0.27 M	0.09 M	–	1 day	20 °C	3	13.18
G3_hc_n	300 ml 1 M[c]	100 ml 1 M	0.75 M	0.25 M	–	1 day	20 °C	3	13.50
G3_hc_mpH_a	300 ml 1 M	100 ml 1 M	0.75 M	0.25 M	5 ml HNO_3	1 day	20 °C	3	13.19
G3_hc_lpH_a	300 ml 1 M	100 ml 1 M	0.75 M	0.25 M	10 ml HNO_3	1 day	20 °C	3	12.62
G1_hc_hpH[d]	50 ml 1 M	50 ml 1 M	0.16 M	0.16 M	20 ml 10 M NaOH	1 day	20 °C	1	13.64
G2_hc_lpH_n	200 ml 1 M	100 ml 1 M	0.67 M	0.33 M	–	1 day	20 °C	2	11.97
G2.8_hc_hpH_n	280 ml 1 M	100 ml 1 M	0.73 M	0.26 M	–	1 day	20 °C	2	13.46
G5_hc_hpH_a	200 ml 1 M	40 ml 1 M	0.8 M	0.16 M	10 ml HNO_3	1 day	20 °C	3	13.40

[a] 'G' stands for gel; the number after 'G' refers to the initial Si/Al; 'l' indicates low; 'm' indicates medium and 'h' indicates high while 'c' signifies concentration; ice represents 'ice bath'; 'n' indicates no NaOH solution while 'a' indicates adding HNO_3. For example, 'G3_hc_lpH_a' represents a gel with an initial Si/Al ratio of 3, using a high concentration of reactants, synthesized at relatively low pH, with the addition of HNO_3.
[b] The pH of filtrate referring to 25 °C. The measurement is detailed in Section 2.2.
[c] Note that it is not possible to prepare 2 M (or higher) of silicate solution at room temperature due to the matter of solubility.
[d] Extra 200 ml of deionized water was added to this mixture to obtain pure N-A-S-H gel, as a concentrated mixture with low Si/Al tends to form Al-containing phases.

dispersed on a carbon adhesive tape and coated with carbon prior to the analysis. Secondary electron images were acquired with magnifications of 5000× and a working distance of 10 mm. The area of the images was scanned with a spot size of 5.0 and a dead time of 10 %. TGA data were recorded on a thermoanalyzer TG-449-F3-Jupiter instrument on ~10 mg samples at a heating rate of 10 °C/min from 40 to 1000 °C, except in the middle stage staying at 105 °C for 6 h in order to determine the amount of non-evaporable water in N-A-S-H gel.

For the filtrate, its pH was determined by measuring the concentration of OH^- by titration against 0.1 M HCl. The concentration of Si, Al and Na were measured by a Perkin Elmer Optima 5300 DV ICP-OES spectrometer. Mass balance calculations, based on the initial solution composition and the measured concentrations of Al and Si, were also used to estimate the Si/Al ratio of the gel.

2.3. Solubility measurement

The synthesized "high pH" N-A-S-H gels as detailed in section 3.3 were re-dispersed into deionized water with a solid-to-water ratio of 20 g/l in a nearly full vessel containing only a small fraction of air. The batch reactor was tightly sealed to minimize carbonation. According to previous investigations [13,14], the dissolution of N-A-S-H gel and zeolite at room temperature can be expected to be at near equilibrium after around 1 month, i.e. no significant variations of their solubility products will occur after >1 month. Thus, the dissolution test in this work was conducted in a rotator at a speed of 220 rpm and equilibrated for 2 months at 25 °C, and for 1 month at 40 and 60 °C. Then, the suspensions were filtered to separate the solid and aqueous phases. For each sample, triplicate measurements were performed and the average results are presented.

The solid residue was freeze-dried until a constant weight was obtained. The dried solid residue, obtained from the dissolution test at 60 °C, was subjected to XRD analysis to determine if any phase transition had occurred during the dissolution process. The pH of the filtrate was measured with a pH meter at room temperature and then corrected with the Gibbs free energy minimization program GEM-Selektor V3 (GEMS) [20] for the pH difference caused by difference from room temperature to 40 °C: −0.58 and to 60 °C: −0.98. The total concentrations of Si, Al and Na in the filtrate were measured by ICP-OES with a Perkin Elmer Optima 5300 DV spectrometer.

2.4. Thermodynamic modeling

GEMS was employed to determine the solubility product and thermodynamic properties of N-A-S-H gels. The PSI/Nagra [21] and Cemdata18 [22] thermodynamic databases were used for the thermodynamic data of solid, aqueous, and gaseous phases.

The activity of a species, $\{i\}$, was calculated with GEMS from the measured concentration (m_i) using $\{i\} = \gamma_i \bullet m_i$, where γ_i is the activity coefficient and can be computed using the built-in extended Debye-Hückel equation in GEMS:

$$log\gamma_i = \frac{-A_y z_i^2 \sqrt{I}}{I + B_y a_i \sqrt{I}} + b_y I \quad (1)$$

where z_i is the charge of species i, I is the effective molal ionic strength, A_y and B_y are P,T-dependent coefficients, a_i is the ion size parameter, which is set at 3.31 Å for all charged ions for NaOH-based solution, and b_y is a semi-empirical parameter (~0.098 for NaOH solutions at 25 °C) [22]. The activity of water was also calculated.

Based on the solubility products determined, the Gibbs free energy of

reaction, $\Delta_r G^0$, and thus the Gibbs free energy of formation $\Delta_f G^0$ can be calculated according to Eq. (2):

$$\Delta_r G^0 = -RTlnK_{sp} = \sum_i \nu_i \Delta_f G_i^0 \quad (2)$$

where R is the universal gas constant, 8.3145 J/mol/K, T represents absolute temperature in K, ν_i is the stoichiometric reaction coefficient, $\Delta_f G_i^0$ stands for the Gibbs free energy of formation of the species used in the reaction.

The apparent Gibbs free energy of formation at any desired temperature $\Delta_a G_T^0$ can be calculated according to Eq. (3):

$$\Delta_a G_T^0 = \Delta_f G_{T_0}^0 - S_{T_0}^0 (T - T_0) + \int_{T_0}^{T} C_P^0 dT - \int_{T_0}^{T} \frac{C_P^0}{T} dT \quad (3)$$

where $T_0 = 298.15$ K, $\Delta_f G_{T_0}^0$ refers to the Gibbs free energy of formation at 298.15 K, $S_{T_0}^0$ denotes the standard entropy at 298.15 K, while C_P^0 corresponds to the standard heat capacity. A more detailed description of the derivation of the dependence of the Gibbs free energy on temperature can be found in [23]. Since C_P^0 can be assumed to remain constant within the narrow temperature range of 20–80 °C [14,23,24], Eq. (3) can be simplified to

$$\Delta_a G_T^0 = \Delta_f G_{T_0}^0 - S_{T_0}^0 (T - T_0) + C_{T_0}^0 \left(Tln\frac{T}{T_0} - T + T_0 \right) \quad (4)$$

Standard values of heat capacity C_p^0 and entropy S^0 were estimated using the additivity method [23,25] ($\Delta_r C_p^0 = 0$ *or* $\Delta_r S^0 = 0$) from C_p and S° and the molar volume of faujasite Y ($Na_2Al_2Si_4O_{12}{\cdot}8H_2O$), quartz and zeolitic H_2O, using the following Eq. (5). Furthermore, the entropy term was further corrected for volume changes according to Eq. 62 in [26], which found that accounting for volume changes enhanced the accuracy of the entropy correction.

$$\Phi^0_{(Na_2O)_a(Al_2O_3)_a(SiO_2)_b(H_2O)_c} = a\Phi^0_{Na_2Al_2Si_4O_{12}\bullet 8H_2O} + (2b - 4a)\Phi^0_{SiO_2} + (c - 8a)\Phi^0_{H_2O} \quad (5)$$

where Φ^0 represents C_p^0 or S^0. The thermodynamic data of components are provided in Table A2.

To assess the accuracy of C_p^0 or S^0, the solubility product $logK_T$ at different temperatures were calculated using the 3-term extrapolation function [27] (see Eq. (6)) in GEMs, to compare to the experimentally determined $logK_T$.

$$logK_T = a + \frac{b}{T} + c\ lnT \quad (6)$$

where

$$a = \left[\Delta S_{T_0}^0 - \Delta C_{p,T_0}^0 (1 + lnT_0) \right] / 2.303R$$

$$b = (-\Delta H_{T_0}^0 + \Delta C_{p,T_0}^0 T_0) / 2.303R$$

$$c = \Delta C_{p,T_0}^0 / 2.303R$$

T_0 represents the temperature at 298.15 K, ΔS and ΔC_P denote the changes in entropy and heat capacity of the reaction at T_0.

The values of the standard molar volume V^0 were also estimated using the additivity method using Eq. (7). The molar volumes of the components used in Eq. (7) have been optimized in [28] as also detailed in Table A2.

$$V^0_{(Na_2O)_a(Al_2O_3)_a(SiO_2)_b(H_2O)_c} = aV^0_{Na_2O} + bV^0_{SiO_2} + aV^0_{Al_2O_3} + cV^0_{H_2O} \quad (7)$$

3. Results and discussion

3.1. Verification of the existing sol-gel method

Table 2 summarizes the obtained Si/Al ratios in synthesized N-A-S-H gels derived from different initial Si/Al in this work and from the literature. The Si/Al ratios of the synthesized N-A-S-H gels obtained by XRF and mass balance calculation in this work remained at around 1, even if the initial Si/Al increased from 1 to 3. The maximum Si/Al ratio achieved (1.9) with mixture G10 was still low, although the initial Si/Al ratio corresponded to 10. Similar results and trends were observed in [11], as also shown in Table 2. They found that the obtained Si/Al ratio could only increase if the Si/Na ratio was also increased, resulting in lower pH values. For instance, the obtained Si/Al ratio increased from 1.1 to 2.4, when Si/Na ratio increased from 0.1 to 1.1 and the initial Si/Al ratio increased from 0.9 to 9.6. This indicates that the concentration of Na, and thus the pH, has a significant influence on the obtained Si/Al ratio. The results from this work and from [11] both show that the obtained Si/Al value in the solid is much lower than its corresponding initial Si/Al, except for the case of initial Si/Al = 1. The Si/Al ratios obtained by XRF are consistent with those calculated by mass balance, indicating the results are reliable.

Table 2
Obtained Si/Al ratio of synthesized N-A-S-H gels from this work and literature.

	G1	G2	G3	G10
Initial Si/Al	1	2	3	10
Obtained Si/Al by XRF	1.05 ± 0.01	1.13 ± 0.01	1.33 ± 0.01	1.89 ± 0.02
Obtained Si/Al by mass balance	1.06	1.36	1.39	1.97
Literature Si/Al by mass balance	0.98 [11]	1.10 [11]	–	2.39 [11]
Literature Si/Al by EDX	1.45 [17], 1.11 [12]	2.19 [17], 2.08 [12]	–	–
Literature Si/Al by NMR	1.36 [17]	1.62 [17]	–	–

In contrast, Si/Al ratios in N-A-S-H gels near the target Si/Al of 1 and 2 were obtained by [12,17]. This might be partially related to the measurement technique (see Table 2) but maybe also to the different synthesis conditions. An ice bath was employed in [17] to lower the reaction temperature, while the reaction time was extended to 7 days in [12]. Hence, the effect of reaction temperature and reaction time was further revealed by comparing mixtures G3, G3_ice and G3_7days. As observed from Table 3, lower temperature (G3_ice) slightly increased the obtained Si/Al ratio from 1.33 to 1.46, while the extension of reaction time from 1 day (G3) to 7 days (G3_7days) hardly affected the Si/Al ratio of the N-A-S-H gel.

The structure of the synthesized N-A-S-H gel was also characterized by XRD (Fig. 1) and FTIR (Fig. 2). The broad XRD humps at around 30° 2θ indicate that, in fact, only amorphous N-A-S-H gels had formed. Note that the XRD hump of amorphous SiO_2 is centered at around 20° 2θ, which is not observed on the obtained gels. G3_ice and G10 were slightly carbonated due to unavoidable contact with air during the post-treatment of samples. No significant shift of this broad XRD peak was observed with the Si/Al ratio of the N-A-S-H gels, since these N-A-S-H gels were almost identical in chemical composition. According to experimental results in [29] and simulation results in [30], the hump at around 30° 2θ is expected to be shifted to a smaller angle as the Si/Al increases. The XRD results of two synthesized N-A-S-H gels in [12] also look almost identical, indicating a similar Si/Al in these two gels, although the authors claimed that Si/Al in the synthesized N-A-S-H gels, determined by SEM/EDX was around 1 and 2, respectively. The FTIR technique is much more sensitive in detecting structural changes of

Table 3
Effect of reaction temperature and reaction time.

	G3	G3_ice	G3_7days
Initial Si/Al	3	3	3
Obtained Si/Al by XRF	1.33 ± 0.01	1.46 ± 0.01	1.34 ± 0.01
Obtained Si/Al by mass balance	1.39	1.59	1.51

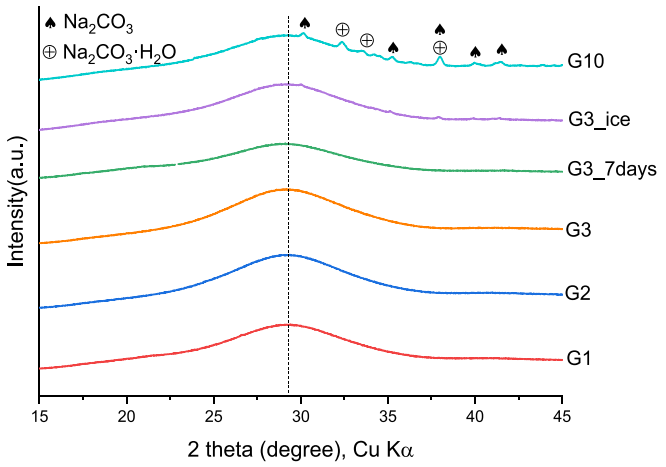

Fig. 1. XRD patterns of N-A-S-H gels synthesized at different initial Si/Al ratios, reaction temperatures and reaction times.

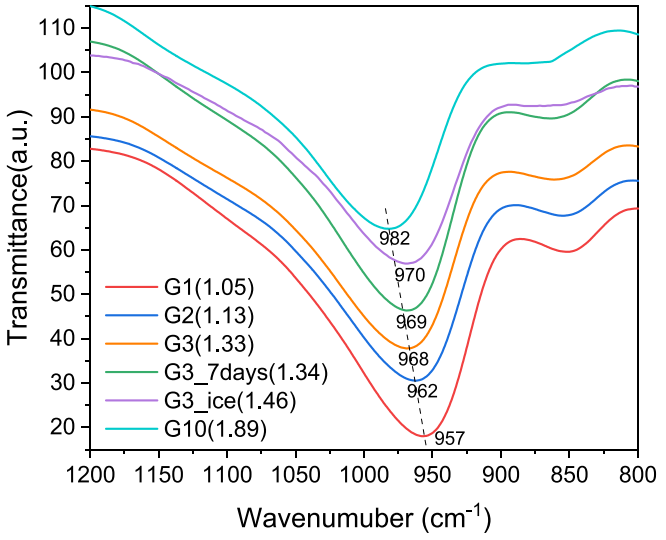

Fig. 2. FTIR spectra of N-A-S-H gels synthesized at different initial Si/Al ratios, reaction temperatures and reaction times. The obtained Si/Al ratio of each sample is indicated in the bracket in the legend (e.g., G1(1.05)).

amorphous aluminosilicates, as it is sensitive to short-range structural order [31]. FTIR spectra of these five synthesized N-A-S-H gels were compared in Fig. 2. The main band centered at around 950–980 cm^{-1} is attributed to asymmetric stretching vibrations of Si–O–T (T refers to Si or Al) bonds. The shift of this band to a higher wavenumber was highly consistent with the corresponding increment of the obtained Si/Al ratio in gels.

The XRD and FTIR results together show only a minor difference among these six synthesized N-A-S-H gels, underlining that the difference in their chemical composition identified by XRF is small. The above results show that it is difficult to synthesize an N-A-S-H gel with a Si/Al ratio of 2 or 3 by using the methods reported in [10,12,16]. Neither increasing the reaction time nor lowering the reaction temperature led to a significant increase in the Si/Al ratio. A strong increase of the initial Si/Al only led to a moderate increase of the final Si/Al ratio, and the obtained Si/Al ratio of 1.9 was much lower than the initial Si/Al ratio of 10 used to prepare sample G10. In a next step, the effect of concentration and pH on the Si/Al ratio in N-A-S-H gel was further studied.

3.2. Modification of mixtures for the synthesis of high Si/Al N-A-S-H gels

3.2.1. The effect of concentration of reactants and pH

Changing the concentration of the reactants or lowering the pH values are options to enable the synthesis of high Si/Al N-A-S-H gels.

In a first step, the pH of the mixing solution was lowered by not adding additional NaOH solution to the mixtures. This resulted in a decrease in the pH value of the filtrate from 13.7 (sample G3) to 12.9 (sample G3_lc_n). Concurrently, the Si/Al ratio rose from 1.3 (sample G3) to 1.8 (sample G3_lc_n), underlining the strong effect of pH as elaborated in more detail later in this discussion.

In a second step, the influence of the concentration of the reactants was investigated, as summarised in Table 4. Increasing the Si concentration in the mixture from 150 to 270, and to 750 mM increased the Si/Al ratio in the N-A-S-H gel from 1.8 to 1.9 and to 2.2, respectively, according to the XRF results. The Si/Al ratios calculated based on mass balance are slightly higher than those obtained by XRF. However, even at the highest concentration of reactants used in this study, the target Si/Al ratio of 3 has not been reached, despite the Si/Al ratio has raised significantly (by about 0.4 after XRF data) from G3_lc_n to G3_hc_n.

Lowering the amount of NaOH, and thus the pH value, is an essential factor for increasing the Si/Al, as indicated by the comparison between G3 and G3_lc_n, whose only difference is the absence of additional NaOH (see Table 1) for the latter. This was further investigated on variants of sample G3_hc_n, where different amounts of HNO_3 were added (see Table 1). Table 5 shows a clear increase of Si/Al in N-A-S-H gels at lower pH values. At pH 12.6, the obtained Si/Al ratio (2.74) is already close to the target Si/Al of 3. To sum up, a high Si/Al ratio of up to 3 could be reached with a combination of using a high concentration of reactants (0.75 M of Si and 0.25 M of Al) and low pH values (<13).

3.2.2. Aqueous solution

The concentrations of reactants and pH are two significant factors affecting the obtained Si/Al ratio in synthesized N-A-S-H gel. Thus the composition of the filtrated solution was analyzed by ICP-OES. The detailed element concentration for all samples is given in the Appendix (Table A3). The difference in the initial and final concentration of Si and Al in the filtrated solution are illustrated in Fig. 3 and Fig. 4. Although the final Si concentration in the filtrated solution increased with the initial Si concentration, a higher percentage of Si was consumed when the initial concentration was higher. This indicates a higher percentage of Si was bound in the solid in the samples with higher initial concentrations and is consistent with the XRF data of the synthesized N-A-S-H gels, where a higher Si/Al was observed (see Table 4). In contrast, >95 % of Al was consumed for all cases, and only a trace amount of Al remained in the solution even at the elevated initial concentration of Al, indicating a high affinity of Al to form solid N-A-S-H gel. For all cases shown in Fig. 3, the proportion between Al and Si in the filtrated solution was far from being equal to the initial proportion, as aqueous Si was significantly higher than the concentration of Al. This means the proportion of Si forming the solid phase is lower than that of Al. As a result, the Si/Al ratio in the N-A-S-H gel was lower than the corresponding initial Si/Al ratio as shown in Table 5. Taking G3_lc_n as an example, 66 % of Si and nearly 100 % of Al was in the solid, such that the resulting Si/

Table 4
Effect of concentration of reactants on the obtained Si/Al ratio.

	G3	G3_lc_n	G3_mc_n	G3_hc_n
Initial Si/Al	3	3	3	3
Obtained Si/Al by XRF	1.33 ± 0.01	1.83 ± 0.02	1.92 ± 0.02	2.23 ± 0.02
Obtained Si/Al by mass balance	1.39	2.00	2.06	2.27

Note: no extra NaOH solution was added in this serial of gels compared to the serial of gels in Tables 2 and 3.

Table 5
Effect of pH on the obtained Si/Al ratio in N-A-S-H gels.

	G3_hc_n	G3_hc_mpH_a	G3_hc_lpH_a
pH	13.50	13.19	12.62
Initial Si/Al	3	3	3
Obtained Si/Al by XRF	2.23 ± 0.02	2.35 ± 0.02	2.74 ± 0.02
Obtained Si/Al by mass balance	2.27	2.48	2.92

Al ratio of 1.8 in the synthesized N-A-S-H is still lower than the target Si/Al of 3. By increasing the concentration of reactants, a greater proportion of Si can be consumed to form N-A-S-H gel, thereby increasing the obtained Si/Al ratio.

Fig. 4 illustrates the effect of pH on the concentration of Si and Al remaining in the solution. Again, a negligible amount of Al was detected in the solution for all samples, suggesting substantial Al consumption. In addition, it's noteworthy that Si concentration significantly increased with elevated pH values. This is attributed to the strong tendency of Si to form negatively charged aqueous complexes under basic pH conditions, including species such as $SiO_4H_3^-$, $SiO_4H_2^{2-}$ and $Si_4O_8(OH)_4^{4-}$ [21], Consequently, in a higher pH environment, Si demonstrates a stronger tendency to persist in solution rather than precipitating into the solid phase. The same tendency has also been observed for Si and Al at increased pH values in the so-called C-A-S-H phases [32]. Note that in all cases, the measured Si concentrations and Al concentrations were well below the solubility of amorphous SiO_2 or microcrystalline $Al(OH)_3$ [21,33] at those pH values, making their formation improbable. Due to the lower solubility of Si at lower pH, more Si is able to form solid N-A-S-H gel. As a result, higher Si/Al ratio can be obtained with decreasing pH, as shown in Table 5. When pH was lowered to 12.6 as in the case of G3_hc_lpH_a, around 97 % of Si and almost 100 % of Al had precipitated and a Si/Al of 2.7, i.e. close to the initial Si/Al of 3 can be achieved.

In summary, the key to obtaining high Si/Al N-A-S-H gel is to ensure that a high fraction of the initial Si precipitates as gel, which depends primarily on a relatively low pH and to a lower extent on higher initial concentrations.

3.2.3. *Optimized route for synthesis of high Si/Al N-A-S-H gels*

Inspired by the success in the case of G3_hc_lpH_a to achieve N-A-S-H gel with a Si/Al ratio near 3, G2_hc_lpH_n was synthesized at a relatively low pH, aiming the obtainment of N-A-S-H gel with a Si/Al ratio of 2. It can be seen from Table 6 that, by using an initial Si/Al ratio of 2 and pH of filtrate of 12.0, the obtained Si/Al, i.e. 1.9, was almost equal to the target Si/Al of 2. Overall, the target Si/Al ratio can be achieved using the same initial Si/Al if pH is carefully adjusted to ensure the major part of Si forms N-A-S-H gel.

Table 6
Two options to synthesize N-A-S-H gels with Si/Al of 2 and 3.

Series	Samples	pH of filtrate	Initial Si/Al	Target Si/Al	Obtained Si/Al by XRF
Mixtures 1	G2_hc_lpH_n	11.98	2	2	1.88 ± 0.02
	G3_hc_lpH_a	12.62	3	3	2.74 ± 0.02
Mixtures 2	G2.8_hc_hpH_n	13.46	2.8	2	1.95 ± 0.02
	G5_hc_hpH_a	13.40	5	3	2.81 ± 0.02

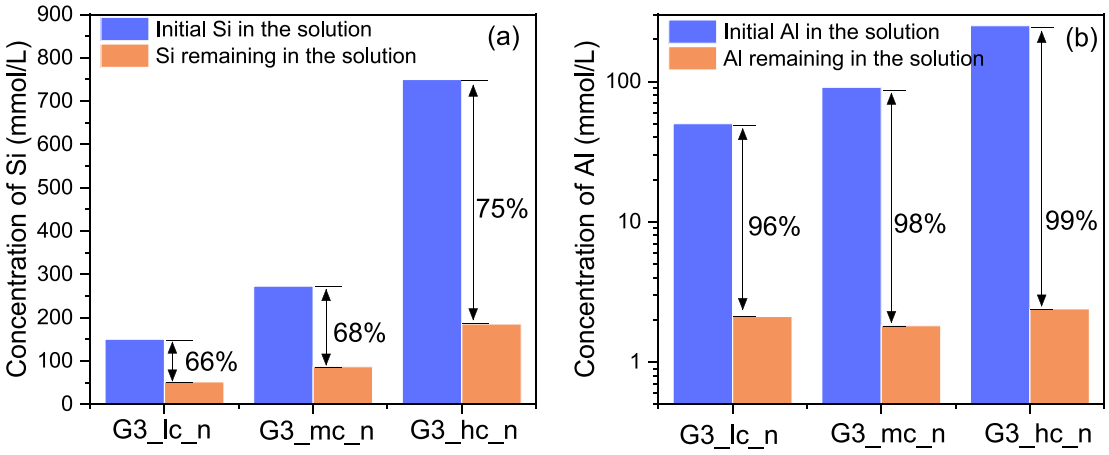

Fig. 3. Effect of concentration of reactants on the reactant consumption.

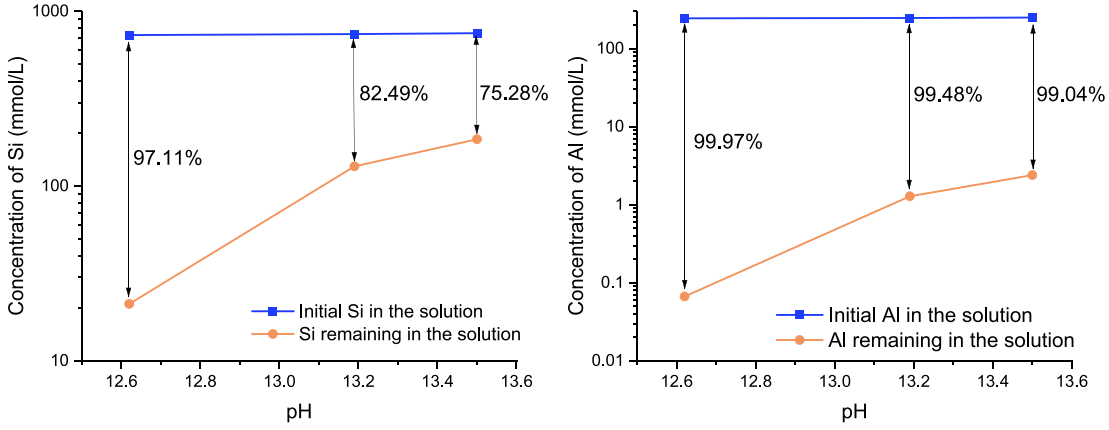

Fig. 4. Effect of pH on the reactant consumption.

The N-A-S-H gel synthesized here at relatively low pH values might be different from the real geopolymer gel formed at much higher pH values. The pH in the pore solution in fly ash-based geopolymer pastes at 28 days ranges from 13.4 to 13.8, based on an initial water-to-binder ratio of 0.35 [34], while in the present study, the final pH values ranged from 12.0 to 12.6. The different conditions needed are mainly related to the amount of water (solution) present. In geopolymer pastes, a very low water-to-solid ratio is generally used, resulting in extremely high initial concentrations (around 10 times as those in sol-gel method). As a result, even at high pH values, substantial amounts of Si and Al will end up in solid phases. In contrast, the sol-gel method employs a high water-to-solid ratio. In this case, pH plays a more dominant role. This is why it is difficult to achieve a Si/Al ratio above 1 at very high pH values using the sol-gel procedure with high water to solid ratios as shown in Section 3.1. To mimic the real environment in the pore solution of geopolymer paste, it would be better to synthesize N-A-S-H gel at high pH values, which means the initial Si/Al ratio has to be considerably higher than the target Si/Al ratio. For instance, an initial Si/Al ratio of 2.8 (mixture G2.8_hc_hpH_n) was needed to obtain N-A-S-H gel with a final Si/Al of 2 at a pH of 13.46. To obtain a Si/Al of 2.8, an initial Si/Al of 5 was needed. Note that pH is closely linked with the initial Si/Al ratio when using sodium silicate as Si-providing substance. The higher the initial Si/Al is, the higher the pH and the lower the fraction of silicon in the solid.

3.3. Overview of synthesized N-A-S-H gels at high pH with Si/Al from 1 to 3

Thus, N-A-S-H gels with Si/Al ratios of 1, 2 and 3 were also synthesized successfully at high pH: G1_hc_hpH, G2.8_hc_hpH_n and G5_hc_hpH_a, respectively. In order to maintain a pH level as high as in geopolymer paste, extra NaOH solution was added for Si/Al = 1, nothing to Si/Al = 2 while HNO_3 was added for Si/Al = 3, as detailed in Table 1.

3.3.1. Chemical composition of synthesized high pH N-A-S-H gels

The chemical compositions of three types of synthesized high pH N-A-S-H gels were determined by XRF, SEM/EDX and mass balance, as summarised in Table 7. Fig. A1, A2 and A3 in the Appendix display secondary electron images used to determine the chemical composition of gels obtained with mixtures G1_hc_hpH, G2.8_hc_hpH_n and G5_hc_hpH_a, respectively. The targeted Si/Al ratios, namely 1, 2 and 3, were obtained successfully. Basically, Si/Al ratios obtained by these three techniques are consistent with each other. Although Si/Al ratios obtained SEM/EDX and mass balance are much closer and both of them are slightly higher than those obtained from XRF, XRF is believed to be the most reliable technique to determine the chemical composition. SEM/EDX is generally classified as a semi-quantitative elemental analysis method [35,36], while mass balance calculation is a non-direct method which introduce some additional errors. Na/Al ratios obtained from XRF and SEM/EDX are also very close, but generally a bit above the theoretical expected ratio of 1, regardless of Si/Al. This is probably due to the presence of dissolved Na in the small amount of water associated with the gels. Na/Al ratio from mass balance calculation was not shown because the content of Na could not be reliably quantified.

The amount of non-evaporable water was also determined, i.e. the amount of water that cannot be removed by D-drying or equivalent procedures, e.g. drying at 105 °C [37,38]. In this work, drying at 105 °C was selected to determine the dry weight and calculate the amount of non-evaporable water based on TGA measurements. As can be seen from Fig. 5, the mass of all samples decreased during drying at 105 °C until a constant mass loss (< 0.1 %/h) was reached at 6 h, corresponding to the loss of evaporable water. Subsequently, the temperature was increased at a rate of 10 °C/min up to 1000 °C, resulting in a mass loss of around 5 %, which was assigned to the loss of non-evaporable water in the N-A-S-H gels. It is generally believed that N-A-S-H gels contain relatively little non-evaporable water [39]. According to the TGA results, the stoichiometric coefficient m in synthesized N-A-S-H gels, $(Na_2O)_1(SiO_2)_{1-3}(Al_2O_3)_1(H_2O)_m$, ranges from 1 to 1.5. Rahier et al. [40] reported an even lower m of 0.4 in a geopolymer gel $(Na_2O)_1(SiO_2)_{3.4}(Al_2O_3)_1(H_2O)_m$. This difference is probably due to the low liquid/solid ratio used during the reaction of sodium silicate and metakaolin [40], while the sol-gel procedure presented here used a high liquid/solid ratio, indicating that N-A-S-H gel formed in geopolymers could contain less non-evaporable water than N-A-S-H gel synthesized by the sol-gel method. In terms of comparison with synthesized N-A-S-H gel in the literature, Gomez-Zamorano et al. [12] reported an even higher stoichiometry factor m of 5 to 8 for $(Na_2O)_1(SiO_2)_{1-2}(Al_2O_3)_1(H_2O)_m$ and Williamson et al. [11] reported an m value of 4–5 for $(Na_2O)_1(SiO_2)_1(Al_2O_3)_1(H_2O)_m$,i.e. values at least ten times larger than those reported for geopolymers [40]. The differences in the values obtained in this work on synthesized gels lies, at least partially, in the temperature range used to determine the non-evaporable water as they considered the total mass loss from 40 or 50 °C to 975 °C [11,12], which overestimates the amount of non-evaporable water by roughly a factor of 3 to 4 as illustrated in Fig. 5. Based on the results of XRF and TGA, the chemical compositions of three types of N-A-S-H gels are listed in Table 8.

3.3.2. Structural characterization of synthesized N-A-S-H gels

The high pH N-A-S-H gels with various Si/Al ratios all exhibited a single amorphous hump in XRD curves, as shown in Fig. 6. The hump shifted towards small angles as Si/Al ratios increased, which is entirely in line with observations in geopolymer pastes [29], where XRD humps at 28.5°, 26.9°, and 26.3° were observed for Si/Al ratios of 1.5, 2.5, 4.5, respectively. It is the first time that an observable shift towards lower 2θ with increasing Si/Al ratio in XRD has been reported for synthesized N-A-S-H gels, indicating a clear difference in the chemical composition. Such a shift was also predicted by molecular dynamics for the XRD patterns of N-A-S-H gels [30], which related it to the more compact structures of N-A-S-H gels with lower Si/Al and thus smaller spacings,

Table 7
Average Si/Al and Na/Al ratios in synthesized N-A-S-H gels.

	G1_hc_hpH	G2.8_hc_hpH_n	G5_hc_hpH_a
$(Si/Al)_{XRF}$	1.10 ± 0.01	1.95 ± 0.02	2.81 ± 0.02
$(Si/Al)_{EDX}$	1.20 ± 0.05	2.17 ± 0.08	3.15 ± 0.10
$(Si/Al)_{Mass\ balance}$	1.17	2.24	3.35
$(Na/Al)_{XRF}$	1.08 ± 0.01	1.18 ± 0.01	1.21 ± 0.01
$(Na/Al)_{EDX}$	1.03	1.15	1.07

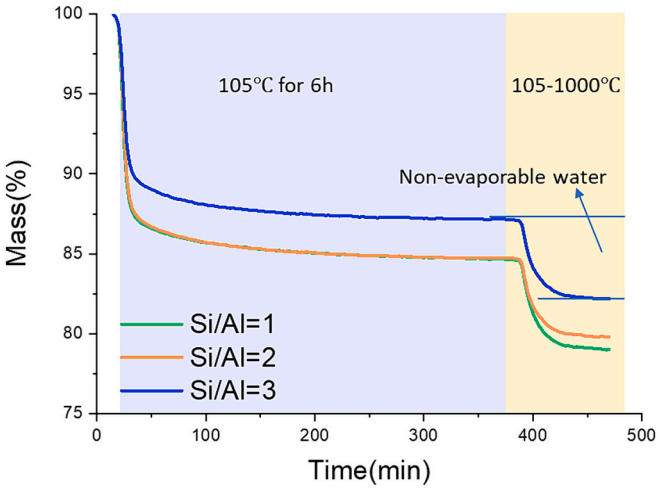

Fig. 5. Thermogravimetric analysis of synthesized N-A-S-H gels at high pH with Si/Al ratios from 1 to 3.

Table 8
Chemical composition of synthesized high pH N-A-S-H gels.

Samples	Non-evaporable water	Chemical composition
Si/Al = 1.1	5.59 %	$(Na_2O)_{1.1}(SiO_2)_{2.2}(Al_2O_3)_1(H_2O)_{0.99}$
Si/Al = 2.0	4.84 %	$(Na_2O)_{1.2}(SiO_2)_4(Al_2O_3)_1(H_2O)_{1.18}$
Si/Al = 2.8	4.90 %	$(Na_2O)_{1.2}(SiO_2)_{5.6}(Al_2O_3)_1(H_2O)_{1.47}$

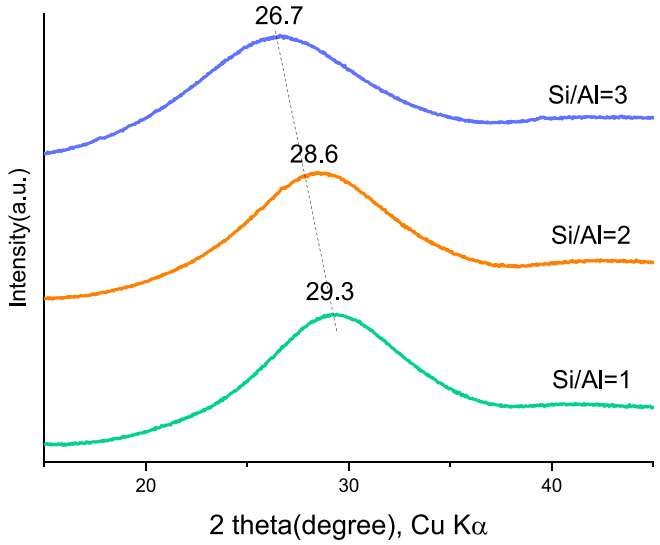

Fig. 6. XRD patterns for synthesized high pH N-A-S-H gels with Si/Al ratios from 1 to 3.

corresponding to larger angles according to Bragg's law.

The FTIR spectra of these synthesized high pH N-A-S-H gels with various Si/Al ratios are shown in Fig. 7. The main band in the region between 1250 and 920 cm^{-1} is attributed to the asymmetric stretching vibrations of Si–O–T (T refers to Si or Al) [41,42]. This band is a typical signal indicating the formation of N-A-S-H gel [43,44]. The position of the main band contains vital information about Si/Al ratio and connectivity of the N-A-S-H gel framework [5,45]. A noticeable shift towards a higher wavenumber is observed as Si/Al increases from 1 to 3, which is related to vibrations of the Si-O-Si band at a higher wavenumber than the Si-O-Al band, due to the stronger electronegativity of Si^{4+} [14] and then higher binding energy of Si-O-Si [46]. The band

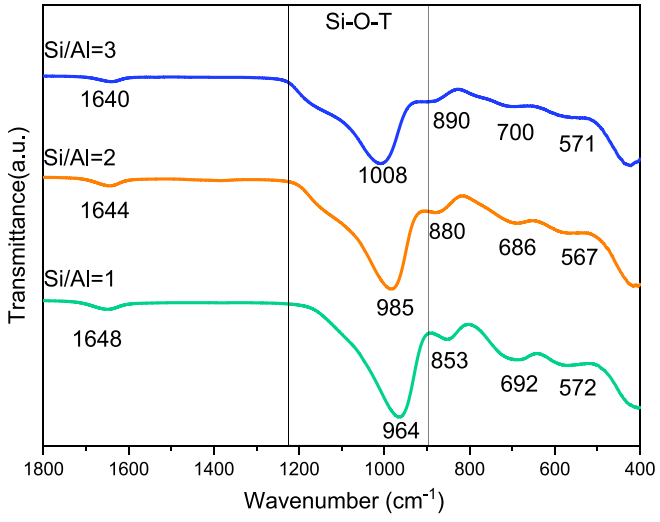

Fig. 7. FTIR spectra for synthesized high pH N-A-S-H gels with Si/Al from 1 to 3.

appearing at 920–800 cm^{-1} is likely associated with asymmetric stretching vibrations of Si–O–Al [6]. The band becomes less pronounced with increasing Si/Al ratio, indicating a lower Si-O-Al link fraction. A similar trend was observed as the Si/Na increased in [47]. The band centered at around 690 cm^{-1} is assigned to symmetrical stretch vibrations of Si–O–T [6,48]. A weak band at around 570 cm^{-1} is contributed by the ring vibration of the TO_4 tetrahedron [6]. The weak nature of the band is due to the absence of crystalline phases [5]. Finally, the band located at around 1640 cm^{-1} is corresponding to the bending vibration of H-O-H [14,49]. Overall, the wavenumbers and the amount of IR bands for each N-A-S-H gel were in good agreement with those in literature [6,44]. Based on the above chemical composition and structural information, it can be concluded that the target N-A-S-H gels with various Si/Al ratios from 1 to 3 were successfully synthesized.

The structural properties of N-A-S-H gel, according to the above XRD and FTIR results, are closely related to the chemical composition i.e. Si/Al. Fig. 8 summarizes the positions of XRD humps and Si-O-T asymmetric stretching bands for all synthesized N-A-S-H gels with various Si/Al ratios. A clear decreasing trending of 2θ angle with increasing Si/Al ratio can be observed, indicating a larger basal spacing. A linear increase of the wavenumber for Si-O-T stretching band is found with increasing Si/Al ratio in Fig. 8(b). This linear relationship suggests the shift of Si-O-T stretching band, and can be a reliable signal to access the Si/Al ratio in N-A-S-H gel. The near linear shift of the XRD and FTIR bands with the Si/Al indicates indirectly also that there is little difference in the structure between N-A-SH samples synthesized at low or high pH values or high or low initial concentrations.

3.4. Solubility products of N-A-S-H gels

The analysis of the XRD patterns of the N-A-S-H gels after re-equilibration at 60 °C confirmed that the gel remained amorphous and had not transformed to any crystalline phases at high temperature, as shown in Fig. A4 in the Appendix. In addition, the XRD patterns of the solid residue remain the same peak shift with Si/Al ratio as those observed before dissolution test. The concentrations of different elements and the pH in the filtrated solution after dissolution are also provided in the Appendix (Table A4). The solubility products of N-A-S-H gels at different temperatures were calculated based on the dissolution reactions listed in Table 9. Note that the chemical compositions of the N-A-S-H gel are slightly modified to achieve a Na/Al ratio of 1, assuming that the slight surplus of Na observed by EDS and XRF is due to the presence of some water with a high concentration of Na. Fig. 9 shows the log K_{sp} values of the synthesized N-A-S-H gels with different Si/Al ratios, as well as literature values derived from the dissolution reactions using the same species, i.e. Na^+, AlO_2^-, SiO_2^0 and OH^- (if necessary for charge balance). For those utilizing different species in their calculations, a transformation was made to facilitate comparison, as shown in Table A1. It can be seen that the log K_{sp} values of N-A-S-H gels increase with temperature, indicating a greater solubility at a higher temperature. For N-A-S-H gel with Si/Al ratios of 1.1 and 2.0 synthesized in this work, it was found that their log K_{sp} values are very close to those of the amorphous N-A-S-H gels in Williamson et al. [11] and Gomez-Zamorano et al. [12]. However, the N-A-S-H gel synthesized by Walkley et al. [13] exhibit less negative log K_{sp} values. This may be partly because of the lower Na content assumed in the N-A-S-H gel by Walkley et al. [13]. Additionally, the N-A-S-H gel in [13] was obtained via alkali activation of synthetic glass instead of the sol-gel method, which could be another reason for the discrepancy.

Since N-A-S-H gel can be regarded as a disordered form of zeolite, especially of the ABC-6 family of zeolites [50], it is worth to compare their solubility products to explore the effect of crystallinity. Hydroxysodalite ($Na_8Al_6Si_6O_{24}(OH)_2{\cdot}2H_2O$), a member of the ABC-6 family, and Gismondine: LS-P ($Na_2Al_2Si_2O_8{\cdot}3.8H_2O$) [14] as well as faujasite [11] are selected to compare with N-A-S-H gel with a Si/Al ratio of 1, while faujasite Y ($Na_2Al_2Si_4O_{12}{\cdot}8H_2O$) [14], also belonging to ABC-6

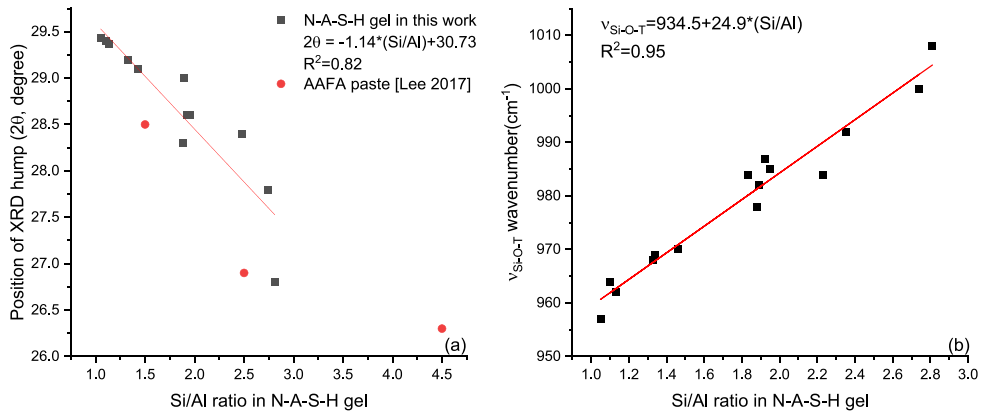

Fig. 8. Correlation between (a) position of XRD hump and Si/Al in N-A-S-H gel and (b) wavenumber of Si-O-T asymmetric stretching vibrations in FTIR and Si/Al in N-A-S-H gel.

Table 9
Dissolution reactions used to calculate solubility products per 1 mol of Si.

N-A-S-H gels	Dissolution reactions
Si/Al = 1.1	$(Na_2O)_{0.46}(Al_2O_3)_{0.46}(SiO_2)_1(H_2O)_{0.48} \rightarrow 0.92\ Na^+ + 0.92\ AlO_2^- + SiO_2^0 + 0.48\ H_2O$
Si/Al = 2.0	$(Na_2O)_{0.25}(Al_2O_3)_{0.25}(SiO_2)_1(H_2O)_{0.29} \rightarrow 0.5\ Na^+ + 0.5\ AlO_2^- + SiO_2^0 + 0.29\ H_2O$
Si/Al = 2.8	$(Na_2O)_{0.18}(Al_2O_3)_{0.18}(SiO_2)_1(H_2O)_{0.26} \rightarrow 0.36\ Na^+ + 0.36\ AlO_2^- + SiO_2^0 + 0.26\ H_2O$

family, were chosen for comparison with N-A-S-H gel with a Si/Al ratio of 2. The log K_{sp} values of these zeolites from [11,14] are also plotted in Fig. 9 after normalization to 1 mol of Si. It can be seen from Fig. 9 that all types of zeolites (empty symbols) have lower log K_{sp} values compared to the amorphous N-A-S-H gels (filled symbols), indicating that the gels have a higher solubility. This is reasonable as zeolites have a crystalline structure that is considered more stable and less likely to dissolve than amorphous gels. Similar results were also found in [11], where a clear decrease of from N-A-S-H gel with Si/Al = 1 to faujasite was observed. The log K_{sp} value of hydroxysodalite is the smallest, with several log K_{sp} units smaller than N-A-S-H gel with a Si/Al ratio of 1. This is because it contains extra Na^+ and OH^- compared with the chemical composition of N-A-S-H gel with a Si/Al ratio of 1 in this work, which lowers the log K_{sp} value mathematically if normalized to 1 Si. In contrast, the log K_{sp} value of faujasite Y is only around 1 log K_{sp} unit more negative than N-A-S-H gel with a Si/Al ratio of 2, implying that N-A-S-H gel might have an atomic structure similar to that of faujasite.

To study the effect of the Si/Al ratio on the solubility product of N-A-S-H gel, the log K_{sp} values should be normalized to the same number of framework TO_4, i.e., $SiO_4 + AlO_4$. Both the log K_{sp} values of N-A-S-H gel from this work and from [12] exhibit an increasing trend with an increase in Si/Al ratio, as can be seen in Fig. 10. This is partly because of lower Na content in higher Si/Al N-A-S-H gel, even at constant TO_4, which means a smaller stoichiometric coefficient is used for Na to calculate the solubility products (see Table 9) resulting in less negative log K_{sp} value due to purely mathematical reasons. However, it should be noted that in this study, the magnitude of the increase in the log K_{sp} value with Si/Al ratio is notably different between the Si/Al ratios of 1 to 2 and 2 to 3, with a more significant increase observed in the latter range. This indicates that the formation of N-A-S-H gel with a high Si/Al ratio is thermodynamically less favoured. This is also supported by the molecular dynamic simulation result in [30], which reported that the Si/Al ratio of the constructed N-A-S-H gel model was <3, regardless of the Si/Al ratio in the initial configuration. Furthermore, it could help explain why the synthesis of N-A-S-H gel with a Si/Al ratio up to 3 is challenging and has previously not been reported in literature.

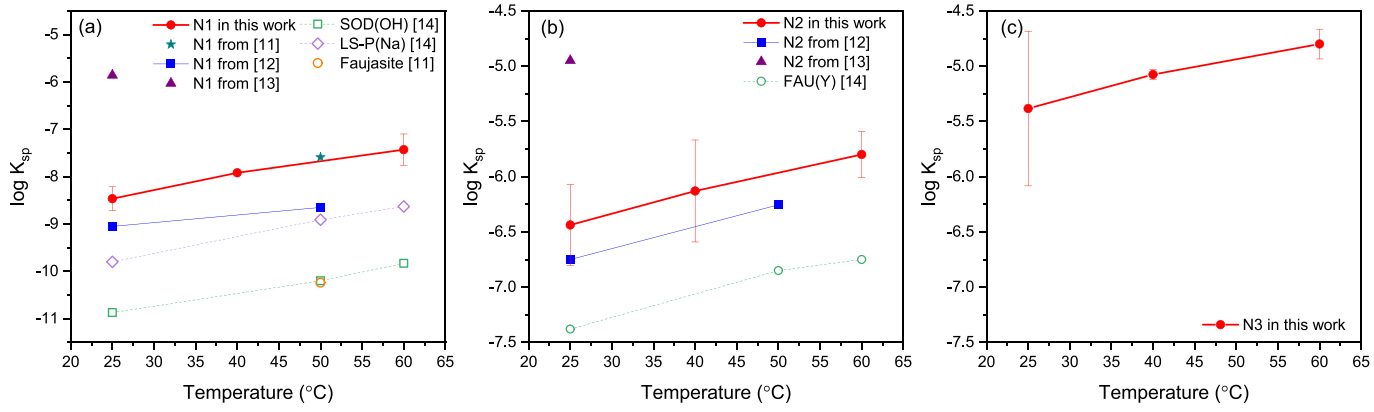

Fig. 9. Log solubility products of synthesized N-A-S-H gels (filled symbols) and zeolites (empty symbols) normalized to 1 mol of Si, (a) Si/Al ratio = 1, (b) Si/Al ratio = 2, (c) Si/Al ratio = 3. Error bars correspond to the two sided 95 % confidence interval. Literature data for N-A-S-H derived from [11–13] and for zeolites (Faujasite, sodalite and gismondine (LS-P(Na)) from [11,14]).

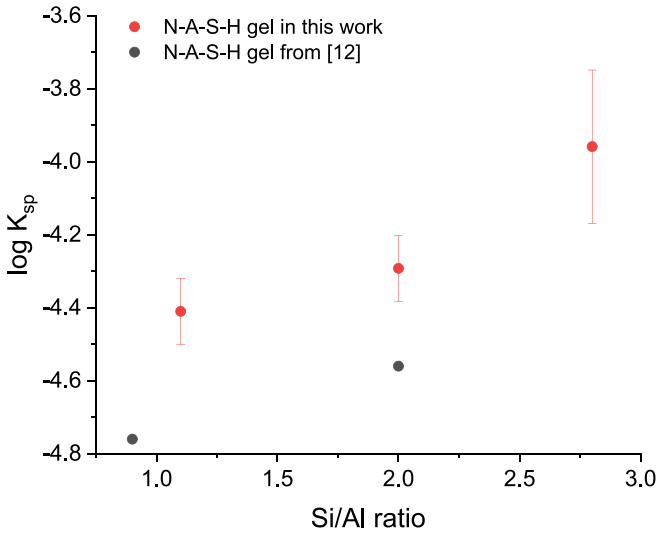

Fig. 10. Effect of Si/Al ratio on log solubility products of synthesized N-A-S-H gels normalized to 1 mol of (SiO_4 + AlO_4) at 25 °C. Error bars correspond to the two sided 95 % confidence interval. Black dots from [12].

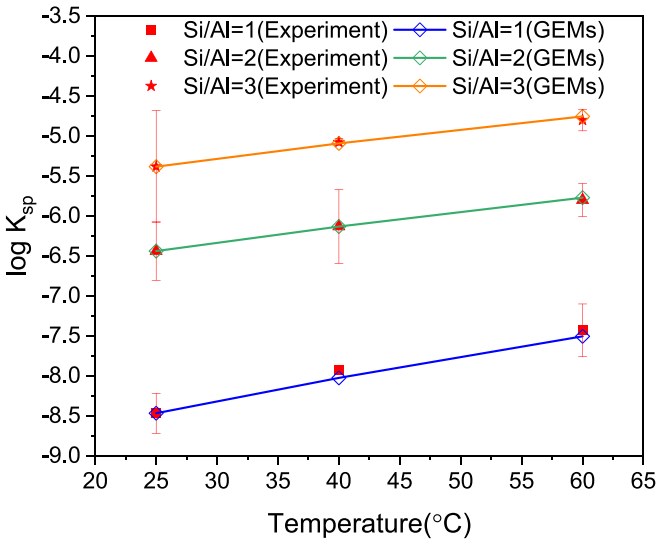

Fig. 11. Comparison between the measured solubility products, log K_{sp}, and the temperature extrapolations from thermodynamic modeling using the data summarised in Table 10. Error bars correspond to the two sided 95 % confidence interval.

3.5. Thermodynamic properties of N-A-S-H gels

Based on the measured log K_{sp} values at 25 °C, the Gibbs free energy of formation $\Delta_f G^0$ of N-A-S-H gels at 25 °C was calculated as detailed in Eq. (2). The heat capacity C_p^0, entropy S^0 and molar volume V^0 of the N-A-S-H gels were estimated using the additivity method according to Eq. (5) and Eq. (7). And finally the enthalpy $\Delta_f H^0$ of N-A-S-H gels was obtained from the Gibbs free energy and the entropy. The thermodynamic properties of N-A-S-H gels with various Si/Al ratios at 25 °C are shown in Table 10.

The changes in the solubility products with temperature depend on the differences in the heat capacity C_p^0 and entropy S^0 between the species in solution and the N-A-S-H gels as detailed in Eq. (6). To evaluate the accuracy of C_p^0 and S^0 calculated in this work, the solubility products of N-A-S-H gels, derived through Eq.(6), were compared with experimental results, as illustrated in Fig. 11. In agreement with the experimental observations, the solubility increases with temperature. The log K_{sp} values calculated via Eq.(6) describe the experimentally measured data well, indicating that the estimated heat capacity C_p^0 and entropy S^0 data of the N-A-S-H gels are in a reasonable range.

4. Conclusion

In this work, N-A-S-H gels with Si/Al ratios ranging from 1 to 3 were synthesized using a newly developed sol-gel method. The effects of reaction temperature, reaction time, initial Si/Al ratio, reactant concentrations and pH values in the solution on the final Si/Al in synthesized N-A-S-H gels have been systematically studied. The chemical and structural information of N-A-S-H gels were characterized using XRF, SEM/EDX, TGA, XRD and FTIR analysis, as well as mass balance calculation. A thermodynamic database of N-A-S-H gels with various Si/Al ratios has been established. The following conclusions can be drawn:

(1) The existing mixtures and reaction conditions for sol-gel methods reported in the literature have been found to produce N-A-S-H gel with Si/Al ratio near 1, even at high initial Si/Al in the mixing solutions. It was found that changing the reaction temperature, the reaction time or the initial Si/Al had little effect on the Si/Al ratio in the N-A-S-H gel.

(2) The key approach to obtain N-A-S-H gel with a high Si/Al ratio was to lower the pH values and to use more concentrated solutions. Decreasing the pH value under basic conditions lowers the tendency of Si to remain in the solution because of its aqueous speciation, thereby allowing a higher Si/Al ratio in the N-A-S-H gel. This poses a challenge for the synthesis of high Si/Al N-A-S-H gels at very high pH, e.g. in the range of the alkalinity of pore solutions in geopolymers. To achieve it, an initially Si/Al ratio higher than target must be employed.

(3) N-A-S-H gels exhibit varying structures depending on their Si/Al ratios, as evidenced by XRD and FTIR patterns. The XRD humps of N-A-S-H gels clearly shift with changes in the Si/Al ratio. Moreover, the FTIR results can be utilized to determine the Si/Al ratio in N-A-S-H gel based on the position of stretching the Si-O-T band.

(4) The solubility products of N-A-S-H gels with Si/Al ratios of 1 and 2 are in good agreement with those reported in the literature [12], and higher than those of zeolites with the same Si/Al ratios, thus indicating a higher solubility of N-A-S-H gels. The solubility product of N-A-S-H gels with a Si/Al ratio of 3 has been determined for the first time and is much less negative than those with lower Si/Al ratios, indicating that the formation of N-A-S-H gel with high Si/Al ratio is thermodynamically little favoured.

(5) The temperature dependent solubility products of N-A-S-H gels derived from estimated heat capacity and entropy data agree closely with the experimentally observed trends. This result supports the validity of the thermodynamic properties of N-A-S-H gels determined in this work.

Table 10
Standard thermodynamic properties of N-A-S-H gels at 25 °C.

N-A-S-H gels	$\Delta_f G^0$ (kJ/mol)	$\Delta_f H^0$ (kJ/mol)	S^0 (J/mol/K)	C_p^0 (J/mol/K)	V^0 (cm^3/mol)
$Na_{0.92}Al_{0.92}Si_1O_{3.84}{\cdot}0.48H_2O$	−1997.78	−2151.46	83	150	33.51
$Na_{0.5}Al_{0.5}Si_1O_3{\cdot}0.29H_2O$	−1483.63	−1590.74	75	103	22.19
$Na_{0.36}Al_{0.36}Si_1O_{2.72}{\cdot}0.26H_2O$	−1317.96	−1416.39	57	89	18.93

CRediT authorship contribution statement

Yun Chen: Conceptualization, Investigation, Methodology, Writing – original draft. **Luiz Miranda de Lima:** Conceptualization, Investigation, Methodology. **Zhenming Li:** Writing – review & editing. **Bin Ma:** Methodology, Writing – review & editing. **Barbara Lothenbach:** Methodology, Writing – review & editing. **Suhong Yin:** Supervision. **Qijun Yu:** Supervision. **Guang Ye:** Supervision, Writing – review & editing.

Declaration of competing interest

The authors declare the following financial interests/personal relationships which may be considered as potential competing interests: Yun Chen reports financial support was provided by China Scholarship Council.

Data availability

Data will be made available on request.

Acknowledgments

The first author would like to acknowledge China Scholarship Council (Grant No. 201906150022) for financial support in this work. The third author would like to acknowledge Guangdong Provincial Key Laboratory of Intelligent and Resilient Structures for Civil Engineering (2023B1212010004).

Appendix A. Supplementary data

Supplementary data to this article can be found online at https://doi.org/10.1016/j.cemconres.2024.107484.

References

[1] J.L. Provis, S.A. Bernal, Geopolymers and related alkali-activated materials, Annu. Rev. Mater. Res. 44 (2014) 299–327, https://doi.org/10.1146/annurev-matsci-070813-113515.
[2] C. Ruiz-Santaquiteria, J. Skibsted, A. Fernández-Jiménez, A. Palomo, Alkaline solution/binder ratio as a determining factor in the alkaline activation of aluminosilicates, Cem. Concr. Res. 42 (2012) 1242–1251, https://doi.org/10.1016/j.cemconres.2012.05.019.
[3] S. Das, P. Yang, S.S. Singh, J.C.E. Mertens, X. Xiao, N. Chawla, N. Neithalath, Effective properties of a fly ash geopolymer: synergistic application of X-ray synchrotron tomography, nanoindentation, and homogenization models, Cem. Concr. Res. 78 (2015) 252–262, https://doi.org/10.1016/j.cemconres.2015.08.004.
[4] A. Palomo, S. Alonso, A. Fernández-Jiménez, Alkaline activation of fly ashes: NMR study of the reaction products, J. Am. Ceram. Soc. 87 (2004) 1141–1145. https://ceramics.onlinelibrary.wiley.com/doi/pdf/10.1111/j.1551-2916.2004.01141.x (accessed May 10, 2019).
[5] C.A. Rees, J.L. Provis, G.C. Lukey, J.S.J. Van Deventer, Attenuated total reflectance fourier transform infrared analysis of fly ash geopolymer gel aging, Langmuir 23 (2007) 8170–8179, https://doi.org/10.1021/la700713g.
[6] B. Walkley, R. San Nicolas, M.A. Sani, J.D. Gehman, J.S.J. Van Deventer, J. L. Provis, Phase evolution of Na2O-Al2O3-SiO2-H2O gels in synthetic aluminosilicate binders, Dalton Trans. 45 (2016) 5521–5535, https://doi.org/10.1039/c5dt04878h.
[7] F. Pacheco-Torgal, J. Castro-Gomes, S. Jalali, Alkali-activated binders: a review: part 1. Historical background, terminology, reaction mechanisms and hydration products, Constr. Build. Mater. 22 (2008) 1305–1314, https://doi.org/10.1016/J.CONBUILDMAT.2007.10.015.
[8] M.R. Rowles, B.H. O'Connor, Chemical and structural microanalysis of aluminosilicate geopolymers synthesized by sodium silicate activation of metakaolinite, J. Am. Ceram. Soc. 92 (2009) 2354–2361, https://doi.org/10.1111/j.1551-2916.2009.03191.x.
[9] T. Bakharev, Geopolymeric materials prepared using class F fly ash and elevated temperature curing, Cem. Concr. Res. 35 (2005) 1224–1232, https://doi.org/10.1016/j.cemconres.2004.06.031.
[10] T. Williamson, J. Han, L. Katz, G. Sant, M. Juenger, Method for experimentally determining N-A-S-(H) solubility, RILEM Tech. Lett. 3 (2019) 104–113, https://doi.org/10.21809/rilemtechlett.2018.63.
[11] T. Williamson, L.E. Katz, J. Han, H.A. Dobbs, B.F. Chmelka, G. Sant, M.C. G. Juenger, Relationship between aqueous chemistry and composition, structure, and solubility of sodium aluminosilicate hydrates, J. Am. Ceram. Soc. 103 (2020) 2160–2172, https://doi.org/10.1111/jace.16868.
[12] L. Gomez-Zamorano, M. Balonis, B. Erdemli, N. Neithalath, G. Sant, C–(N)–S–H and N–A–S–H gels: compositions and solubility data at 25°C and 50°C, J. Am. Ceram. Soc. 100 (2017) 2700–2711, https://doi.org/10.1111/jace.14715.
[13] B. Walkley, X. Ke, O. Hussein, J.L. Provis, Thermodynamic properties of sodium aluminosilicate hydrate (N-A-S-H), Dalton Trans. (2021), https://doi.org/10.1039/d1dt02202d.
[14] B. Ma, B. Lothenbach, Synthesis, characterization, and thermodynamic study of selected Na-based zeolites, Cem. Concr. Res. 135 (2020) 106111, https://doi.org/10.1016/j. cemconres.2020.106111.
[15] A. Fernández-Jiménez, A. Palomo, Composition and microstructure of alkali activated fly ash binder: effect of the activator, Cem. Concr. Res. 35 (2005) 1984–1992, https://doi.org/10.1016/j.cemconres.2005.03.003.
[16] G.V.P. Bhagath Singh, K.V.L. Subramaniam, Influence of processing temperature on the reaction product and strength gain in alkali-activated fly ash, Cem. Concr. Compos. 95 (2019) 10–18, https://doi.org/10.1016/j.cemconcomp.2018.10.010.
[17] I. García-Lodeiro, A. Fernández-Jiménez, A. Palomo, D.E. MacPhee, Effect of calcium additions on N-A-S-H cementitious gels, J. Am. Ceram. Soc. 93 (2010) 1934–1940, https://doi.org/10.1111/j.1551-2916.2010.03668.x.
[18] I. García-Lodeiro, A. Fernández-Jiménez, M.T. Blanco, A. Palomo, FTIR study of the sol-gel synthesis of cementitious gels: C-S-H and N-A-S-H, J. Sol-Gel Sci. Technol. 45 (2008) 63–72, https://doi.org/10.1007/s10971-007-1643-6.
[19] K. Scrivener, R. Snellings, B. Lothenbach, A Practical Guide to Microstructural Analysis of Cementitious Materials, 2018, https://doi.org/10.1201/b19074.
[20] D.A. Kulik, T. Wagner, S.V. Dmytrieva, G. Kosakowski, F.F. Hingerl, K. V. Chudnenko, U.R. Berner, GEM-Selektor geochemical modeling package: revised algorithm and GEMS3K numerical kernel for coupled simulation codes, Comput. Geosci. 17 (2013) 1–24, https://doi.org/10.1007/s10596-012-9310-6.
[21] T. Thoenen, W. Hummel, U. Berner, E. Curti, The PSI/Nagra Chemical Thermodynamic Database 12/07, 2014.
[22] B. Lothenbach, D.A. Kulik, T. Matschei, M. Balonis, L. Baquerizo, B.Z. Dilnesa, G. D. Miron, M. R, Cemdata18: a chemical thermodynamic database for hydrated Portland cements and alkali-activated materials, Cem. Concr. Res. (2019) 472–506, https://doi.org/10.1109/ICCPS.2014.6843714.
[23] G.M. Anderson, D.A. Crerar, Thermodynamics in Geochemistry: The Equilibrium Model, Oxford University Press, Oxford, 1993.
[24] B. Lothenbach, E. Bernard, U. Mäder, Zeolite formation in the presence of cement hydrates and albite, Phys. Chem. Earth 99 (2017) 77–94, https://doi.org/10.1016/j.pce.2017.02. 006.
[25] B. Lothenbach, T. Matschei, G. Möschner, F.P. Glasser, Thermodynamic modelling of the effect of temperature on the hydration and porosity of Portland cement, Cem. Concr. Res. 38 (2008) 1–18, https://doi.org/10.1016/j.cemconres.2007.08.017.
[26] H.C. Helgeson, J.M. Delany, H.W. Nesbitt, D.K. Bird, Summary and critique of the thermodynamic properties of rock-forming minerals, Am. J. Sci. 278 (1978) 1–229.
[27] D.A. Kulik, Aqueous solubility diagrams for cementitious waste stabilization systems: II, end-member stoichiometries of ideal calcium silicate hydrate solid solutions, J. Am. Ceram. Soc. 84 (2001) 3017–3026, http://scholar.google.com/scholar?hl=en&btnG=Search&q=intitle:Aqueous+Solubility+Diagrams+for+Cementitious+Waste#7.
[28] L. Glasser, The effective volumes of waters of crystallization & the thermodynamics of cementitious materials, Cement 3 (2021) 100004, https://doi.org/10.1016/j.cement.2021.10 0004.
[29] B. Lee, G. Kim, R. Kim, B. Cho, S. Lee, C.M. Chon, Strength development properties of geopolymer paste and mortar with respect to amorphous Si/Al ratio of fly ash, Constr. Build. Mater. 151 (2017) 512–519, https://doi.org/10.1016/j.conbuildmat.2017.06.078.
[30] Y. Chen, J.S. Dolado, S. Yin, Q. Yu, A molecular dynamics study of N–A–S–H gel with various Si/Al ratios, J. Am. Ceram. Soc. (2022) 1–13, https://doi.org/10.1111/jace.18597.
[31] W.K.W. Lee, J.S.J. Van Deventer, The effects of inorganic salt contamination on the strength and durability of geopolymers, Colloids Surfaces A Physicochem. Eng. Asp. 211 (2002) 115–126, https://doi.org/10.1016/S0927-7757(02)00239-X.
[32] Y. Yan, B. Ma, G.D. Miron, D.A. Kulik, K. Scrivener, B. Lothenbach, Al uptake in calcium silicate hydrate and the effect of alkali hydroxide, Cem. Concr. Res. 162 (2022), https://doi.org/10.1016/j.cemconres.2022.106957, 1069 57.
[33] B. Lothenbach, L. Pelletier-Chaignat, F. Winnefeld, Stability in the system CaO-Al2O3-H2O, Cem. Concr. Res. 42 (2012) 1621–1634, https://doi.org/10.1016/j.cemconres.2012.09.002.
[34] Y. Zuo, M. Nedeljković, G. Ye, Pore solution composition of alkali-activated slag/fly ash pastes, Cem. Concr. Res. 115 (2019) 230–250, https://doi.org/10.1016/j.cemconres.2018.10.010.
[35] A.S. De Vargas, D.C.C. Dal Molin, A.C.F. Vilela, F.J. Da Silva, B. Pavão, H. Veit, The effects of Na2O/SiO2 molar ratio, curing temperature and age on compressive strength, morphology and microstructure of alkali-activated fly ash-based geopolymers, Cem. Concr. Compos. 33 (2011) 653–660, https://doi.org/10.1016/j.cemcon-comp.2011.03.006.
[36] K. Beltrán-Jiménez, D. Gardner, S. Kragset, K.F. Gebremariam, O.A.M. Reales, M. W. Minde, M.I.L. de Souza, J.A. Aasen, H.J. Skadsem, L. Delabroy, Cement properties characterization from a section retrieved from an oil production well after 33 years of downhole exposure, J. Pet. Sci. Eng. 208 (2022) 109334, https://doi.org/10.1016/j.petrol.2021.109 334.
[37] H.F.W. Taylor, Cement Chemistry, 1998, https://doi.org/10.1016/S0958-9465(98)00023-7.

[38] H.J.H. Brouwers, The work of powers and Brownyard revisited: part 1, Cem. Concr. Res. 34 (2004) 1697–1716, https://doi.org/10.1016/j.cemconres.2004.05.031.
[39] M.C.G. Juenger, F. Winnefeld, J.L. Provis, J.H. Ideker, Advances in alternative cementitious binders, Cem. Concr. Res. 41 (2011) 1232–1243, https://doi.org/10.1016/j.cemconres.2010.11.012.
[40] H. Rahier, B. Van Mele, M. Biesemans, J. Wastiels, X. Wu, Low-temperature synthesized aluminosilicate glasses: part I. Low-temperature reaction stoichiometry and structure of a model compound, J. Mater. Sci. 31 (1996) 71–79, https://doi.org/10.1007/BF00355128.
[41] M. Criado, A. Fernández-Jiménez, A. Palomo, Alkali activation of fly ash: effect of the SiO2/Na2O ratio. Part I: FTIR study, Microporous Mesoporous Mater. 106 (2007) 180–191, https://doi.org/10.1016/j.micromeso.2007.02.055.
[42] Z. Zhang, H. Wang, J.L. Provis, Quantitative study of the reactivity of fly ash in geopolymerization by FTIR, J. Sustain. Cem. Mater. 1 (2012) 154–166, https://doi.org/10.1080/21650373.2012.752620.
[43] C.A. Rees, J.L. Provis, G.C. Lukey, J.S.J. Van Deventer, In situ ATR-FTIR study of the early stages of fly ash geopolymer gel formation, Langmuir 23 (2007) 9076–9082, https://doi.org/10.1021/la701185g.
[44] I. Garcia-Lodeiro, A. Palomo, A. Fernández-Jiménez, D.E. MacPhee, Compatibility studies between N-A-S-H and C-A-S-H gels. Study in the ternary diagram Na2O-CaO-Al2O3-SiO2-H2O, Cem. Concr. Res. 41 (2011) 923–931, https://doi.org/10.1016/j.cemconres.2011.05.006.
[45] A. Hajimohammadi, J.L. Provis, J.S.J. Van Deventer, Effect of alumina release rate on the mechanism of geopolymer gel formation, Chem. Mater. 22 (2010) 5199–5208, https://doi.org/10.1021/cm101151n.
[46] A. Fernández-Jiménez, A. Palomo, Mid-infrared spectroscopic studies of alkali-activated fly ash structure, Microporous Mesoporous Mater. 86 (2005) 207–214, https://doi.org/10.1016/j.micromeso.2005.05.057.
[47] D. Dimas, I. Giannopoulou, D. Panias, Polymerization in sodium silicate solutions: a fundamental process in geopolymerization technology, J. Mater. Sci. 44 (2009) 3719–3730, https://doi.org/10.1007/s10853-009-3497-5.
[48] W.R. Taylor, Application of infrared spectroscopy to studies of silicate glass structure: examples from the melilite glasses and the systems Na2O-SiO2 and Na2O-Al2O3-SiO2, Proc. Indian Acad. Sci. - Earth Planet. Sci. 99 (1990) 99–117, https://doi.org/10.1007/BF02871899.
[49] P. Rożek, M. Król, W. Mozgawa, Spectroscopic studies of fly ash-based geopolymers, Spectrochim. Acta-Part A Mol. Biomol. Spectrosc. 198 (2018) 283–289, https://doi.org/10.1016/j.saa.2018.03.034.
[50] J.E. Oh, P.J.M. Monteiro, S.S. Jun, S. Choi, S.M. Clark, The evolution of strength and crystalline phases for alkali-activated ground blast furnace slag and fly ash-based geopolymers, Cem. Concr. Res. 40 (2010) 189–196, https://doi.org/10.1016/j.cemconres.2009.10.010.